PCCP

Accepted Manuscript

ROYAL SOCIETY OF CHEMISTRY

www.rsc.org/pccp

Probing the 2D confinement on hydrogen dynamics in water and ice adsorbed in graphene oxide sponges†

Giovanni Romanelli,*[a] Roberto Senesi,[ab] Xuan Zhang,[c] Kian Ping Loh,[c] Carla Andreani[a]

We study the single particle dynamics of water and ice adsorbed in graphene oxide (GO) sponges at $T = 293$ K and $T = 20$ K. We use Deep Inelastic Neutron Scattering (DINS) at the ISIS neutron and muon spallation source to derive the hydrogen mean kinetic energy, $\langle E_K \rangle$, and momentum distribution, $n(p)$. Goal of this work was to study the hydrogen dynamics under 2D confinement and the potential energy surface fingerprinting hydrogen interaction with the layered structure of the GO sponge. The observed scattering is interpreted within the framework of the impulse approximation. Both samples of water and ice adsorbed in GO show $n(p)$ functions with almost harmonic and anisotropic line shapes and $\langle E_K \rangle$ values in excess of the values found at the corresponding temperatures in the bulk. The hydrogen dynamics is discussed in the context of the interaction between interfacial water and ice and the confining hydrophilic surface of the GO sponge.

1 Introduction

Significant experimental and theoretical investigations have been addressed to the understanding of the behaviour of water in contact with solid surfaces, at interfaces and, in particular, near hydrophobic surfaces[1–8]. The strong interest in the study of microscopical properties of water confined at the nanoscale is motivated by the importance and role played by such an ubiquitous solvent in many biological processes[9–18], such as for example the dynamics and function of membranes or the structure of ion channel[19]. The emerging picture indicates a significant perturbation of both structural and dynamical properties of water at the fluid-solid interfaces[20]: the hydrophobic surface strongly influences structure and dynamics, especially of interfacial molecules, as compared to bulk liquid[21,22]. In particular, water wetting on a hydrophobic surface at ambient conditions is disallowed by the non-wetting nature of the surface and high vapour pressure of water. The structural perturbation is mainly characterized by an inhomogeneous local density distribution whereas the dynamics shows an increasing anisotropic behaviour in translational and rotational molecular motions.

Graphene oxide (GO) is a nonstoichiometric compound[23] of great interest for proposed application for battery electrodes[24,25] and membrane models[26–28]. Previous work on GO has shown that graphene monolayers can be used to sandwich a layer of water film, which remains trapped in vacuum and high temperature due to the impermeability of graphene, thus allowing an opportunity to study the molecular structure and dynamics of water under superheated or supercritical conditions[29]. This study showed how a sprinkle of graphene oxide nanoflakes on graphene is effective in condensing water nanodroplets and seeding ice epitaxy at ambient conditions, with observation of complex interplay of ionic and non-ionic intercations. By controlling relative humidity and nanoflake density, the formation of a complete ice wetting layer is slowed down to a time scale of 20 hours. This presented an unprecedented opportunity to visualize ice nucleation and growth in real time, and at the molecular level, which can be performed, using non-contact atomic force microscopy[30]. Elucidation of the local environment of hydrogen in water and ice is particularly relevant due to the interplay between the crucial role of protons in hydrogen bonding and the perturbation induced by the two dimensional (2D) confining substrates. In particular the understanding of hydrogen bonding dynamics in GO is important due to its technological relevance of the material. As an example the pH-sensitive graphene oxide composite hydrogel has been made and utilized for selective drug release at physiological pH[31].

In this paper we present results of a Deep inelastic neutron scattering (DINS) study, using neutrons with high momentum, $\hbar q$, and energy transfers, $\hbar\omega$, of the hydrogen dynamics of water and ice 2D- adsorbed in GO lay-

[a] *Università degli Studi di Roma "Tor Vergata", Dipartimento di Fisica and Centro NAST, Via della Ricerca Scientifica 1, 00133 Roma, Italy*

[b] *Consiglio Nazionale delle Ricerche, CNR-IPCF, Sezione di Messina, Italy*

[c] *Graphene Research Centre and Centre for Advanced 2D Materials, Department of Chemistry, National University of Singapore, 3 Science Drive 3, Singapore 117543*

† Electronic Supplementary Information (ESI) available

‡ Current address: ISIS Facility, Rutherford Appleton Laboratory, Chilton, Didcot, Oxfordshire OX11 0QX, United Kingdom; E-mail: giovanni.romanelli@stfc.ac.uk

ered sponges at T= 293 K and T = 20 K. Information about the water hydrogen dynamics is crucial for the understanding of structure of carbon monolayers as well as the intercalation process. A FTIR characterization of the dry GO sponges show that its hydrogen amount is indeed very small (for details see the Electronic Supplementary Information (ESI)). This guarantees that the hydrogen dynamics probed in the present work arises from the adsorbed water only.

DINS probes the quantum behaviour of atomic nuclei directly through the single-particle momentum distribution, $n(p)$, and the mean kinetic energy, $\langle E_K \rangle$. These quantities fingerprint the nuclear quantum effects determined by the properties of the ground state[33,34]. In the case of ice or water, chemical interactions occurring in the bulk typically represent small changes in the energy of constituents, compared to the energy sequestered in the zero-point motion of the protons, primarily in that of the stretching mode. Nuclear quantum effects significantly impact both structure and dynamics and zero-point energy changes as the structure of the hydrogen bond network changes. Thus because of the non-commuting character of position and momentum operators in quantum mechanics, the $n(p)$ is a sensitive probe to the hydrogen local environment as well as a direct measurement of its dynamics[33,35–38,40]. It is important to emphasize the difficulty in obtaining similar information regarding the proton dynamics by other techniques such a Inelastic Neutron Scattering (INS) or Infrared (IR). In these cases they fingerprint different properties related to the vibrational transitions from the ground state to the first excited states[39]. Thus the $n(p)$ measured via DINS is the only quantity which probes the underlying potential energy surface that the hydrogen in water sees as the local environment changes and water adapts its hydrogen-bonding network in response to a 2D confinement in GO sheets.

The DINS technique, also known as Neutron Compton Scattering (NCS)[33,41] probes time-scale regimes of the order of attosecond, *i.e.*, $10^{-15} - 10^{-17}$ s, where scattering is entirely incoherent, *i.e.*, a time window much shorter than the time constants characteristic of the typical collective excitations, typically well above 10^{-15} s[42].

The basic principles of data interpretation of DINS technique are based on the validity of the Impulse Approximation (IA)[43] which is exact in the limit of infinite momentum transfer[44,45]. Within the IA, the inelastic neutron scattering cross-section directly probes the $n(p)$ of all nuclei in the target system and elucidates its connection with the underlying potential energy surface[33]. The $n(p)$ line-shape fingerprints details of the 2D confining potential energy surface that the protons experience in contact with the GO surface, directly reflecting the structure of their local environment. DINS results complement information which is garnered from diffraction techniques that measure the spatial correlations among the nuclear positions. From the results of the analysis of the DINS data, we are able to capture the proton dynamics of water and ice adsorbed in GO and obtain new information on the potential energy surface experienced by the proton. Section II illustrates DINS experiments and data analysis. In Section III, results are presented and discussed. Conclusions are reported in Section IV.

2 Experiment

DINS measurements have been performed at the ISIS neutron and muon spallation source (Rutherford Appleton Laboratory, Chilton, Didcot, UK) on the inverse geometry spectrometer VESUVIO[41,46,47] that uses neutrons with incident energies in the range 1 eV - 10^4 eV. The experiment was performed on hydrated samples of water and ice adsorbed in dry GO sponges contained in an Al container at two different temperatures: at T= 293 K and at T= 20 K at ambient pressure. The sample with water fully absorbed in the GO sponge had a total weight of 1.340 g. Weights of the hydrated sample, *i.e.*, the adsorbed water and the dry GO were 1.172 g and 0.168 g, respectively, corresponding to approximately 87 wt% of adsorbed water. Sample preparation material, detailed description of operation of VESUVIO instrument and data analysis are described in ESI).

The neutron scattering function in the IA regime, $S_{\mathrm{IA}}(q,\omega)$ is expressed in term of the West scaling variable[43] by:

$$\frac{\hbar q}{m} S_{\mathrm{IA}}(\mathbf{q},\omega) = J_{\mathrm{IA}}(y,\hat{\mathbf{q}}) = \int n(\mathbf{p}) \delta\left(y - \mathbf{p}\cdot\hat{\mathbf{q}}\right) \mathrm{d}\mathbf{p} \quad (1)$$

where m is the mass of the particle being struck by the neutron,

$$y_m = \frac{m}{\hbar q}\left(\omega - \frac{\hbar q^2}{2m}\right) \quad (2)$$

the projection of the particle momentum distribution $n(\mathbf{p})$ along the $\hat{\mathbf{q}}$ direction, and $J_{\mathrm{IA}}(y,\hat{\mathbf{q}})$ is the neutron Compton Profile (NCP)[33]. When the sample is isotropic, the particle momentum distribution only depends on the modulus of $\mathbf{p}$, and the $\hat{\mathbf{q}}$ direction is immaterial, so the NCP is simply $J_{\mathrm{IA}}(y) = 2\pi \int_{|y|}^{\infty} p n(p) \mathrm{d}p$. This ideal peak profile, measured in a DINS experiment, is broadened by finite-q correction terms $\Delta J(y,q)$, and by convolution

For consistency with previous literature and ease of notation we write the momentum as a wave vector.

with the instrumental resolution function $R(y,q)$, so the experimental NCP, $F(y,q)$, yields:

$$F(y,q) = [J_{\rm IA}(y) + \Delta J(y,q)] \star R(y,q), \qquad (3)$$

with $\Delta J(y,q) \propto \frac{\partial^3}{\partial y^3} J_{\rm IA}(y)$ (as described in the ESI) and $R(y,q)$ determined using Monte Carlo routines available on VESUVIO.

3 Data analysis and discussion

The primary goal of this experiment was to derive the $J(y)$ line-shape from the $F(y,q)$ spectra and subsequently calculate $n(p)$ and $\langle E_K \rangle$ of the adsorbed water's hydrogens. GO substrates are particularly favourable in these respects, in that the hydrogen amount in the dry GO sponges is very small, as confirmed by the results of the FTIR characterization; DINS measurements of the dry GO sponges confirm this finding: the hydrogen signal from the dry GO is negligible as compared to the hydrated samples (see Figure 8 in ESI for details). This guarantees that DINS measures the dynamics of the protons in the H_2O adsorbed in the GO sponge only. A global fit of the individual $F(y,q)$ spectra, recorded for the angles in forward scattering, was accomplished using two parametric models: (a) a model-independent line-shape, hereafter named Model 1 (M1) and (b) a three dimensional anisotropic Gaussian line-shape derived from a quasi-harmonic model, hereafter named Model 2 (M2). The latter was most recently employed for unraveling of the local environment of hydrogen in polycrystalline ice[48] and heavy water[49].

In M1, the momentum distribution is given by the Gauss-Laguerre expansion[35,44,50]

$$n_{M1}(p) = \frac{\exp\left(-\frac{p^2}{2\sigma^2}\right)}{(\sqrt{2\pi}\sigma)^3} \sum_n c_n (-1)^n L_n^{\frac{1}{2}}\left(\frac{p^2}{2\sigma^2}\right), \qquad (4)$$

where $L_n^{\frac{1}{2}}$ are the generalized Laguerre polynomials, and c_n the expansion coefficients from which, together with the standard deviation, σ, one can derive the momentum distribution line-shape.

In M2, the momentum distribution has been modelled using the spherical average of multivariate Gaussian distribution of the form[48]

$$4\pi p^2 n_{M2}(p) = \left\langle \frac{\delta(p-|\mathbf{p}|)}{\sqrt{8\pi^3}\sigma_x\sigma_y\sigma_z} \exp\left(-\frac{p_x^2}{2\sigma_x^2} - \frac{p_y^2}{2\sigma_y^2} - \frac{p_z^2}{2\sigma_z^2}\right)\right\rangle, \qquad (5)$$

where σ_z is along the direction of the H bond, and σ_x and σ_y are in the plane perpendicular the direction of the H

Table 1 Values of the global-fit parameters on experimental measurements for water in GO at T = 293 K and at 20 K

M1		293 K	20 K
σ	[Å^{-1}]	5.01±0.03	4.99±0.03
c_4		0.14±0.01	0.12± 0.1
$\langle E_K \rangle$	[meV]	156.1±2.0	154.9±2.0
M2		293 K	20 K
σ_x	[Å^{-1}]	3.4±0.5	3.5±0.5
σ_y	[Å^{-1}]	4.6±0.5	4.6±0.5
σ_z	[Å^{-1}]	6.4±0.2	6.3±0.2
$\langle E_K \rangle$	[meV]	156.1±2.0	154.9±2.0
$\langle E_K \rangle_x$	[meV]	24± 6	26± 7
$\langle E_K \rangle_y$	[meV]	45± 9	45± 9
$\langle E_K \rangle_z$	[meV]	86±12	84±12

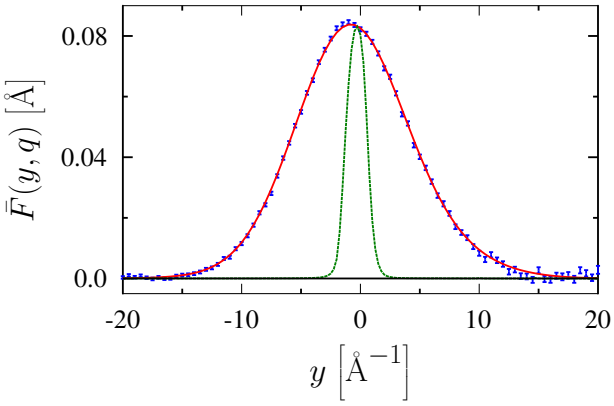

Fig. 1 (color online) Angle averaged hydrogen NCP, $\bar{F}(y,q)$, for water in GO sponges at T = 293 K (blue square with error bars). The fit using M2 is plotted as red line. The experimental resolution $R(y,q)$ is plotted as green line

.

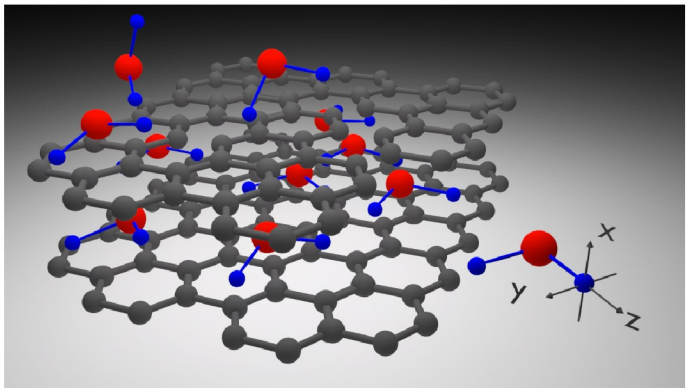

Fig. 2 (color online) Orientation of the water molecules adsorbed on the GO surface and the axis reference system used for the anisotropic model M2

.

bond, *i.e.*, the direction of the maximum value for the zero point energy. The parameter set, $\sigma_{x,y,z}$, determine the anisotropy in the momentum distribution line-shape. Figure 2 reports a sketch showing the orientation of the water molecules adsorbed on the GO surface and the axis reference system used for the anisotropic model M2.

It has to be stressed that although the M1 model represents the most general momentum distribution line-shape, it does not allow to separate the effects of anharmonicity from those of anisotropy[33,51]. Values of the standard deviations σ and σ_α, with $\alpha = x, y, z$, from M1 and M2 models respectively, have been obtained by performing a global fit of the whole set of forward-angle spectra (see SM). Moreover, the hydrogen total mean kinetic energy, $\langle E_K \rangle = 3\frac{\hbar^2\sigma^2}{2m}$, and the directional components along the three spatial axes, $\langle E_K \rangle_\alpha = \frac{\hbar^2\sigma_\alpha^2}{2m}$, have been evaluated and reported in Table 1. From this Table we can appreciate that both M1 and M2 models provide same results for $\langle E_K \rangle$ with little differences in directional $\langle E_K \rangle_\alpha$ values between water and ice. Overall the H dynamics of water and ice confined in 2D GO, exhibits similar three dimensional anisotropy to that found in bulk water[52] and ice[48]. The latter is fingerprinted by the directional components of kinetic energy, $\langle E_K \rangle_\alpha$, with values which are however different with respect to those found in the bulk. The angle-averaged experimental line-shape for DINS data at T=293 K, $\bar{F}(y,q)$, is plotted in Fig. 1 together with fit line-shapes resulting from model M2.

In Table 2 a comparison is made between values for $\langle E_K \rangle$ of present experiment and other DINS experiments on bulk and confined water and ice. These results are consistent with a picture where, for bulk water and ice, the kinetic energy is dominated by the ground state contributions, with the thermal contributions affecting mostly the high-temperature liquid upon approaching the supercritical phase. Differences in the ground state contributions between the solid and the liquid are evident, *i.e.*, the $\langle E_K \rangle$ value of the solid at T= 271 K is about 13 meV higher than the value of the liquid at T= 300 K (see Table 2). Present analysis provides $\langle E_K \rangle$ values for water at T= 293 K and ice at T=20 K 2D confined in GO in excess of 13 meV and 3.7 meV to the corresponding values found in the bulk, respectively. Both values fingerprint the dynamics of water and ice molecules interacting with functional groups on the layers of the GO sponge.

Table 2 The values of the mean kinetic energy resulting from the present experiment (black), compared with previous measurements: Flammini *et al.* (red)[48], Senesi *et al.* (blue)[53], Pantalei *et al.* (magenta)[54], Garbuio *et al.* (green)[6]

Sample	T [K]	$\langle E_K \rangle$ [meV]
Water	423	155.0 ± 3
Water in GO	293	156.1 ± 2.0
Water in Xerogel pores (24 Å)	293	187 ± 3
Water in Xerogel pores (82 Å)	293	156 ± 3
Ice bulk	271	156 ± 2
Water bulk	300	143 ± 3
Ice bulk	71	152.8 ± 2
Ice in GO	20	154.9 ± 2.0
Ice bulk	5	150.9 ±1.5

The plot of radial momentum distributions, $4\pi p^2 n(p)$, corresponding to M2 for water and ice in GO is shown in Fig. 3. The high momentum components in $n(p)$ are highly sensitive to, and dominated by, the curvature of the effective proton potential[54–57], *i.e.*, closely related to the the hydrogen bond strength. The $n(p)$ in a frame attached to an individual water molecule is well described by an harmonic anisotropic Gaussian line-shape, with the transverse momentum width slightly more than one half the width along the stretch mode direction. The tail of the $n(p)$ distributions is due to the momentum along the bond direction, since the proton is most tightly bound in this direction, tight binding implying high momentum width. From Fig. 3 one can appreciate as the momentum width of $n(p)$ line-shape of water adsorbed in GO at T=293 K is clearly expanded, from about 11 Å^{-1}, as compared to bulk water at T=300 K. This finding, similar to what was observed in water at T= 423 K[54] (see Table 2), implies hydrogen bonds are expected to be significantly weaker than in bulk water. The momentum width of $n(p)$ line-shape for ice in GO at T = 20 K extends a little less,

mirroring a OH bond network stronger than in water at T=293 K, although weaker than the value expected for bulk ice at the same temperature.

4 Conclusions

The overall H dynamics of water and ice confined in 2D GO exhibits an anisotropy of the momentum distribution $n(p)$, very much similar to what it is found in bulk water. In GO, water molecules are restrained in layered geometries, with interlayer distances down to 12 Å[58]. This length scale is comparable to the scales of the tethrahedral structural motifs in bulk water. The water response to the perturbation due to this nanometric confinement results in an increase of the hydrogen mean kinetic energy with respect to the bulk. The increase is approximately 13 meV at room temperature and approximately 4 meV at 20 K. Moreover the hydrogen kinetic energy of water in GO shows a negligible temperature dependence, in contrast to the bulk It appears that confinement in GO on one hand induces a higher proton localisation, with increased $\langle E_K \rangle$, and on the other hand preserves the hydrogen dynamics from temperature effects. Likewise, $n(p)$ functions show harmonic anisotropic lineshapes. These findings are ascribed to changes of the proton dynamics induced by the interaction between interfacial water and ice and the confining hydrophilic surface. Due to the negligible DINS signal from the structural hydrogens of the dry GO sponges, the DINS results indicate that changes on $\langle E_K \rangle$ are mainly due to steric confinement and that interactions of water with the functional groups on GO play a negligible role. This result is an important piece of information in view of a thorough understanding of hydrogen bonding dynamics in GO.

Whatever is the origin of the interaction, H dynamics in water confined in 2D GO is quantitatively different from that of water confined in other nanoporous hydrophilic surfaces, such as Xerogel, MCM41 and nanotubes, and unlike any other form of water observed so far. Present results support a picture where the OH bond of water and ice in GO are softer than in bulk water with the energy of the OH expected to be red shifted with a corresponding broadening of the spectral peak.

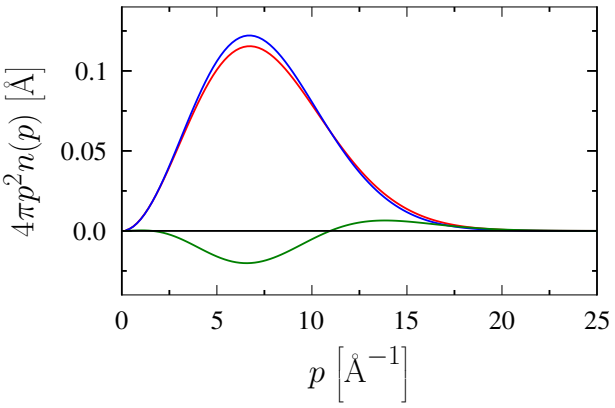

Fig. 3 (color online) $n(p)$ for water in GO sponges at T= 293 K (red line)and bulk water at T= 300 K (blue line); the difference of the two line-shapes, magnified by three times, is plotted as green line

Acknowledgement

This work was supported within the CNR-STFC Agreement No. 06/20018 concerning collaboration in scientific research at the spallation neutron source ISIS. K. P. Loh thanks funding support from NRF Investigatorship Award "Graphene Oxide - A new class of catalytic, ionic and molecular sieving materials NRF12015-01"

References

[1] M. Bellissent-Funel, *Hydration Processes in Biology: Theoretical and Experimental Approaches*, IOS Press, 1999.
[2] O. Mishima and H. E. Stanley, *Nature*, 1998, **396**, 329–335.
[3] C.-Y. Lee, J. A. McCammon and P. J. Rossky, *The Journal of Chemical Physics*, 1984, **80**, 4448–4455.
[4] P. A. Thiel and T. E. Madey, *Surface Science Reports*, 1987, **7**, 211–385.
[5] P. G. Debenedetti, *Journal of Physics Condensed Matter*, 2003, **15**, 1669.
[6] V. Garbuio, C. Andreani, S. Imberti, A. Pietropaolo, G. F. Reiter, R. Senesi and M. A. Ricci, *The Journal of Chemical Physics*, 2007, **127**, 4501.
[7] F. Mallamace, M. Broccio, C. Corsaro, A. Faraone, L. Liu, C.-Y. Mou and S.-H. Chen, *Journal of Physics Condensed Matter*, 2006, **18**, 2285.
[8] C. Pantalei, R. Senesi, C. Andreani, P. Sozzani, A. Comotti, S. Bracco, M. Beretta, P. E. Sokol and G. Reiter, *Physical Chemistry Chemical Physics*, 2011, **13**, 6022–6028.
[9] W. Doster, A. Bachleitner, R. Dunau, M. Hiebl and E. Luscher, *Biophysical Journal*, 1986, **50**, 213–219.
[10] G. Sartor, A. Hallbrucker, K. Hofer and E. Mayer, *The Journal of Physical Chemistry*, 1992, **96**, 5133–5138.

[11] K. Morishige and K. Nobuoka, *The Journal of Chemical Physics*, 1997, **107**, 6965–6969.
[12] S.-H. Chen, P. Gallo and M.-C. Bellissent-Funel, *Canadian Journal of Physics*, 1995, **73**, 703.
[13] J.-M. Zanotti, M.-C. Bellissent-Funel and S.-H. Chen, *Phys. Rev. E*, 1999, **59**, 3084–3093.
[14] L. D. Gelb, K. E. Gubbins, R. Radhakrishnan and M. Sliwinska-Bartkowiak, *Reports on Progress in Physics*, 2000, **63**, 727.
[15] M. C. Bellissent-Funel, S. Longeville, J. M. Zanotti and S. H. Chen, *Phys. Rev. Lett.*, 2000, **85**, 3644.
[16] F. Venturini, P. Gallo, M. A. Ricci, A. R. Bizzarri and S. Cannistraro, *The Journal of Chemical Physics*, 2001, **114**, 10010–10014.
[17] R. Zangi, *Journal of Physics Condensed Matter*, 2004, **16**, 5371.
[18] S.-H. Chen, L. Liu, E. Fratini, P. Baglioni, A. Faraone and E. Mamontov, *Proceedings of the National Academy of Sciences*, 2006, **103**, 9012–9016.
[19] P. G. Debenedetti, *Metastable Liquids: Concepts and Principles*, Princeton University Press, 1997.
[20] D. Chandler, *Nature*, 2005, **437**, 640–647.
[21] J. Marti, G. Nagy, M. C. Gordillo and E. Guàrdia, *The Journal of Chemical Physics*, 2006, **124**, 094703.
[22] G. Nagy, M. C. Gordillo, E. Guàrdia and J. Marti, *The Journal of Physical Chemistry B*, 2007, **111**, 12524–12530.
[23] B. C. Brodie, *Ann. Chim. Phys.*, 1860, **466**, 59.
[24] R. Yazami and P. Touzain, *Synthetic Metals*, 1985, **12**, 499 – 503.
[25] T. Cassagneau and J. H. Fendler, *Advanced Materials*, 1998, **10**, 877–881.
[26] T. Hwa, E. Kokufuta and T. Tanaka, *Phys. Rev. A*, 1991, **44**, 2235.
[27] X. Wen, C. W. Garland, T. Hwa, M. Kardar, E. Kokufuta, Y. Li, M. Orkisz and T. Tanaka, *Nature*, 1992, **355**, 426–428.
[28] F. F. Abraham and M. Goulian, *EPL (Europhysics Letters)*, 1992, **19**, 293.
[29] J. Lu, A. H. C. Neto and K. P. Loh, *Nature Communications*, 2012, **3**, 823.
[30] Y. Zheng, C. Su, J. Lu and K. P. Loh, *Angewandte Chemie International Edition*, 2013, **52**, 8708–8712.
[31] H. Bai, C. Li, X. Wang and G. Shi, *Chem. Commun.*, 2010, **46**, 2376–2378.
[32] H. W. Kim, H. W. Yoon, S.-M. Yoon, B. M. Yoo, B. K. Ahn, Y. H. Cho, H. J. Shin, H. Yang, U. Paik, S. Kwon *et al.*, *Science*, 2013, **342**, 91–95.
[33] C. Andreani, D. Colognesi, J. Mayers, G. F. Reiter and R. Senesi, *Advances in Physics*, 2005, **54**, 377–469.
[34] G. F. Reiter, R. Senesi and J. Mayers, *Phys Rev Lett*, 2010, **105**, 148101.
[35] G. F. Reiter, J. Mayers and J. Noreland, *Phys. Rev. B*, 2002, **65**, 104305.
[36] P. C. Hohenberg and P. M. Platzman, *Physical Review*, 1966, **152**, 198–200.
[37] V. I. Gol'danskii, *Soviet Phys. JETP*, 1957, **4**, 604.
[38] G. K. Ivanov and Y. S. Sayasov, *Soviet Physics Doklady*, 1964, **9**, 171.
[39] A. Parmentier, J. J. Shephard, G. Romanelli, R. Senesi, C. G. Salzmann, and C. Andreani, *The Journal of Physical Chemistry Letters*, 2015, **6**, 2038–2042.
[40] M. Krzystyniak, M. A. Adams, A. Lovell, N. T. Skipper, S. M. Bennington, J. Mayers and F. Fernandez-Alonso, *Faraday Discuss*, 2011, **151**, 171–197.
[41] R. Senesi, C. Andreani, Z. Bowden, D. Colognesi, E. Degiorgi, A. L. Fielding, J. Mayers, M. Nardone, J. Norris, M. Praitano, N. J. Rhodes, W. G. Stirling, J. Tomkinson and C. Uden, *Physica B Condensed Matter*, 2000, **276**, 200–201.
[42] J. M. F. Gunn, C. Andreani and J. Mayers, *Journal of Physics C Solid State Physics*, 1986, **19**, L835–L840.
[43] G. B. West, *Physics Reports*, 1975, **18**, 263–323.
[44] G. Reiter and R. Silver, *Phys Rev Lett*, 1985, **54**, 1047–1050.
[45] G. I. Watson, *J Phys : Condens Matter*, 1996, **8**, 5955–5975.
[46] A. Pietropaolo and R. Senesi, *Physics Reports*, 2011, **508**, 45–90.
[47] J. Mayers and G. Reiter, *Meas Sci Technol*, 2012, **23**, 045902.
[48] D. Flammini, A. Pietropaolo, R. Senesi, C. Andreani, F. McBride, A. Hodgson, M. A. Adams, L. Lin and R. Car, *The Journal of Chemical Physics*, 2012, **136**, 024504.
[49] G. Romanelli, M. Ceriotti, D. E. Manolopoulos, C. Pantalei, R. Senesi and C. Andreani, *The Journal of Physical Chemistry Letters*, 2013, **4**, 3251–3256.
[50] A. Pietropaolo, R. Senesi, C. Andreani, A. Botti, M. A. Ricci and F. Bruni, *Physical Review Letters*, 2008, **100**, 127802.
[51] G. F. Reiter, J. C. Li, J. Mayers, T. Abdul-Redah and P. Platzman, *Brazilian Journal of Physics*, 2004, **34**, 142–147.
[52] C. Andreani, G. Romanelli and R. Senesi, *Chemical Physics*, 2013, **427**, 106–110.
[53] R. Senesi, G. Romanelli, M. Adams and C. An-

dreani, *Chemical Physics*, 2013, **427**, 111–116.

[54] C. Pantalei, A. Pietropaolo, R. Senesi, S. Imberti, C. Andreani, J. Mayers, C. Burnham and G. Reiter, *Phys Rev Lett*, 2008, **100**, 177801.

[55] C. J. Burnham, G. F. Reiter, J. Mayers, T. Abdul-Redah, H. Reichert and H. Dosch, *Physical Chemistry Chemical Physics (Incorporating Faraday Transactions)*, 2006, **8**, 3966.

[56] J. A. Morrone, V. Srinivasan, D. Sebastiani and R. Car, *The Journal of Chemical Physics*, 2007, **126**, 234504.

[57] C. J. Burnham, D. J. Anick, P. K. Mankoo and G. F. Reiter, *The Journal of Chemical Physics*, 2008, **128**, 154519.

[58] A. Buchsteiner, A. Lerf and J. Pieper, *The Journal oo Physical Chemistry B*, 2006, **110**, 22328.